HEATED-WEAPONRY, A PILOT STUDY ON TRACE FORMATION ON HEAT-TREATED SILCRETE

Roné Oberholzer*[1], Veerle Rots[1, 2]

[1] TraceoLab, University of Liège, Belgium

[2] F.R.S.-FNRS, Belgium

*** Correspondence:**
Roné Oberholzer
rone.oberholzer@uliege.be

Place du 20-Août 7, B-4000 Liège, Belgium

Keywords: Silcrete, Traceology, Use-wear, Projectiles, Hafting

Highlight: Use-wear on heat-treated silcrete follows the general 'language' of traceology, but speaks with a unique 'accent' dictated by its heterogeneous structure, necessitating a tailored interpretive framework beyond flint-based models.

Abstract

The Middle Stone Age (MSA) in South Africa features technological innovations such as the intentional heat treatment of silcrete to enhance its knapping properties. Although the importance of heat-treated silcrete in MSA toolkits is acknowledged, there is a notable lack of understanding regarding how use-wear forms and appears on this diverse raw material. This gap results in a shortage of reference data for the functional analysis of archaeological finds, which often depend on models based on uniform materials such as flint. This experimental study examines macro- and micro-use-wear on heat-treated silcrete used in various activities, including projectile work. Findings show that macroscopic wear patterns—such as types of edge fractures—correlate with the hardness of the worked material and the motion involved, generally following the principles known from flint. However, the internal structure of silcrete, consisting of quartz grains embedded in a softer silica matrix, introduces distinctive modifications. Its heterogeneity makes interpreting individual fractures more complex, as their development is influenced by the internal grains. The study concludes that although broad principles of use-wear still apply, heat-treated silcrete displays a unique signature driven by its composite nature. Therefore, analysts should adopt a specialised interpretative approach that goes beyond simple analogies with flint. This research is a crucial step towards creating a comprehensive reference collection for more accurate identification of tool functions on this raw material.

1. Introduction

In South Africa, archaeological finds frequently feature a diverse range of rocks, including quartzite, quartz, hornfels, silcrete, dolerite, and chert. Although silcrete is less commonly recognized in global archaeological studies compared to flint or obsidian, it serves as an essential raw material within South African prehistory. The Middle Stone Age (MSA) in South Africa is marked by the appearance of several innovative behaviours, such as the engraving of ostrich eggshells (Texier et al., 2010), the use of pigments (Hodgskiss, 2020, 2013), bone tool technology(Henshilwood et al., 2001), and personal ornaments(Henshilwood et al., 2004). Silcrete features prominently in at least two significant technological practices. The first is the intentional selection for finer-grained rocks, a pattern associated with the Howiesons Poort segments (Porraz et al., 2013) and Still Bay bifacial points (Henshilwood et al., 2001). The second, innovative behaviour is the deliberate heat treatment of silcrete to alter its physical properties and enhance its flaking quality (Brown et al., 2009; Key et al., 2021; Schmidt et al., 2020). This innovative process has been documented at several key MSA sites, such as Pinnacle Point (Murray et al., 2020), Diepkloof Rock Shelter (Schmidt et al., 2015), Blombos Cave (Mourre et al., 2010a), Nelson Bay cave(Watson, 2025), Klipdrift Rock shelter (Delagnes et al., 2016) and Mertenhof (Schmidt and Mackay, 2016).

The role of heat-treated silcrete in MSA tool kits is well-recognised (Douze et al., 2018; Mourre et al., 2010b; Schmidt et al., 2015; Watson, 2025), yet a significant gap remains in understanding the formation and appearance of use-wear traces on this material. While one investigation confirmed that heat-treated silcrete segments could serve effectively as projectile points, whether hafted transversally or obliquely, it did not provide detailed information on the use-wear traces generated (Schoville et al., 2017). Two studies examined the functionality of heated versus unheated silcrete. Both employed controlled cutting tests, demonstrating that heat treatment significantly enhances the sharpness of the resulting tools (Pargeter and Schmidt, 2020; Toddhunter, 2021). These studies did not provide a detailed analysis of cutting use-wear traces. Although Toddhunter (2021) noted that heat-treated silcrete appears to sustain more edge damage than its unheated counterpart, some studies have examined traces left on silcrete, though most focus on unheated silcrete. These include a study of wear patterns from cutting tubers on various raw materials, including silcrete (Berehowyj, 2013); an investigation of the rate of use-wear formation on silcrete; an experimental comparison of wear patterns on unheated silcrete, porcelain, and glass (Munt et al., 2023); and the creation of a reference collection for silcrete tools used to grind and scrape mineral material (Hilbert et al., 2022). In another study focusing on wear on different materials, they tested the different raw materials across various tasks, including butchering, drilling through light and dense woods, piercing bone and shell, and scraping or adzing wood (Kamminga, 1982) . The results showed that while edge rounding occurred frequently across most activities, the silcrete remained notably resistant to striations.

To begin to understand the development of traces on this rock, we must first examine the rock's nature, which will influence its mechanical properties, and how and where traces form. Silcrete is a hardened duricrust produced by the near-surface silicification of weathered bedrock or sediment. The process creates quartz trapped in a non-quartz matrix, such as clays. This results in a dense framework of original quartz grains embedded within a new silica matrix. Unlike most quartzites, which often break around individual grains, silcrete is sufficiently cohesive that fractures propagate directly through both the grains and the matrix (Webb et al., 2013).

The microtopography of silcrete is very variable and can range from coarse to fine-grained. Before silcrete is heated, it can often be quite coarse-grained and, as a consequence, not have the best knappability. The heat treatment of silcrete enhances its knapping quality by altering its physical and chemical structure—specifically through the loss of SiOH and the formation of new Si–O–Si bonds (Schmidt and Mackay, 2016). At 400 - 500°C there is also a decrease in the volume of pores. It is this decrease in the volume of pores along with the loss of silanole that causes transformation of the flaking properties (Schmidt et al. 2013). These changes reduce fracture toughness, resulting in fracture behaviour similar to that of chert or flint, thereby improving workability and flaking yield (Pargeter and Schmidt, 2020). While past and ongoing studies have focused on how and why silcrete was heat-treated, the formation of use-wear traces on this rock type remains poorly understood. This gap has created a significant shortage of reference material for the analysis of archaeological assemblages.

Functional analysis of wear traces on stone tools primarily depends on experimental reference collections for comparative analysis of archaeological finds. While collections like the TRAIL collection at TraceoLab (University of Liège; Rots, 2021) and others are valuable, they tend to be dominated by homogeneous materials such as flint and obsidian. This leads to a notable gap, since use-wear patterns on these materials may not always be directly relevant to more diverse types of rocks. In response, a growing body of research is now focusing on expanding these collections to include a wider variety of coarse-grained raw materials.

When use-wear on silcrete artefacts is examined, a range of optical microscopy techniques is employed, often applied in combination. Studies typically integrate low-power stereomicroscopy for initial scanning and identification of macro traces, such as edge scarring followed by high-power metallographic microscopy using vertical incident lighting (Berehowyj, 2013; Munt et al., 2023), which is frequently enhanced with Nomarski Differential Interference Contrast (DIC), to facilitate the analysis of micro-polish and striations (Hilbert et al., 2022; Igreja and Porraz, 2013). Some researchers also incorporate hand-held digital microscopes, like a Dino-Lite (Munt et al., 2023), or a Hirox (Hilbert et al., 2022) for documentation, and note that oblique lighting at lower magnifications can clarify certain features, like striations (Munt et al., 2023). A complementary approach involves analysing high-resolution epoxy casts of tool edges to overcome the coarse and reflective nature of the raw material (Igreja and Porraz, 2013). In this process, a negative of the tool edge is made by using polyvinylsiloxane gel, and when this mould has hardened, a mix of epoxy and epoxy hardener is poured in to form the positive that is then studied (Igreja, 2008). Although other non-silcrete studies have observed the negative PVS mould under high magnification vertical incident light without creating a mould (Hayes et al., 2018).

In most reference collections, flint predominates and when use-wear studies were done on silcrete, these collections had to be relied on if reference materials were used. However, the relevance of flint reference frameworks for studying other raw materials has been questioned recently (Taipale et al. *this volume*), despite other researchers arguing in favour (Aleo 2023). Also, a systematic investigation of basalt demonstrated that use-wear formation on this heterogeneous material requires a longer period of use and that the raw material's properties complicate the identification of a clear pattern of micro-wear (Asryan and Rots, 2024). A robust reference framework for silcrete does not yet exist, and the material has not been included in comparative studies. Therefore, we developed an experimental program using heat-treated silcrete for multiple tasks, including projectile activities, and examined macro- and microscopic use-wear traces to begin building a more comprehensive reference framework for silcrete that can be used in the examination of archaeological assemblages.

2. Materials and Methods

2.1 Heat-treatment of silcrete

For this experiment, silcrete from Velddrif, South Africa, was imported. This location was chosen as it still has some quantity of silcrete available from the crop, and it has been identified as a possible fine-grained silcrete source for the nearby site of Diepkloof Rock Shelter (Porraz et al., 2008). Each block of silcrete was numbered, and a flake was removed before heating and labelled with a corresponding number. The silcrete was then heat-treated in a ceramic oven (Colpaert model RHODE). The protocol was adapted from Schmidt et al (2013) and personal communication with Will Archer, who has been involved in several silcrete studies (Archer et al., 2023; Schmidt et al., 2013). In Schmidt et al. 's (2013) paper, they state that the first change in the silcrete is the loss of silanole, which begins at 200-300°C. After this, a temperature between 400 and 500°C must be reached to reduce the volume of pores by 60-80%. The temperature was raised to 450°C over eight hours, maintained at that temperature for four hours, and then allowed to cool naturally for approximately 15 hours within the closed oven (Fig. 1). After the cooling period, the silcrete was removed from the oven, and another flake was struck off to compare with the unheated flakes. Although the exterior textures of the heated blocks were quite similar to before, most had taken on a redder colour. The surfaces of the detached flakes showed a distinct change in texture, visible even macroscopically (Fig. 2). Before heating, the Velddrift silcrete has a coarse, sugary texture and breaks like sandstone, with uneven flake fracture surfaces. After heat-treatment, however, the flaking surfaces were smooth and conchoidal with some larger quartz grains visible in a more homogeneous matrix.

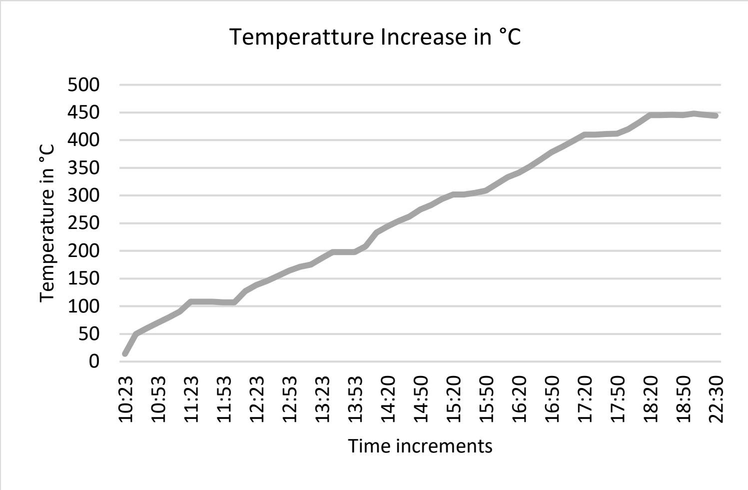

Fig. 1. Chart showing the steady increase in temperature over 10 hours inside the ceramic oven during heating.

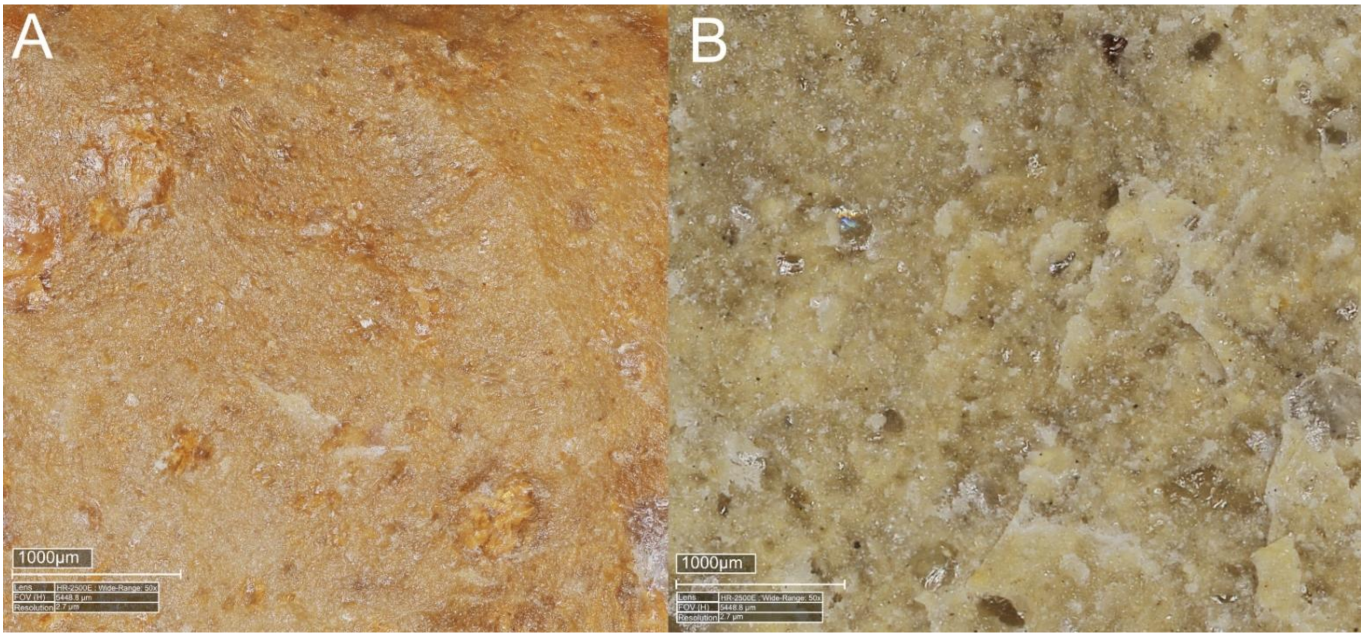

Fig. 2. Fresh fracture surfaces (ventral view) of two silcrete flakes at 50× magnification. Both samples originated from the same block; (A) was removed after heat-treatment and (B) before heat-treatment.

2.2 Experimental tools

The heat-treated silcrete was used to produce a series of backed pieces roughly following the morphology and dimensions of the Howiesons Poort backed pieces of Diepkloof Rock Shelter, South Africa. To create the experimental pieces, we first measured the length, width, thickness, and point angles of the Diepkloof artefacts to establish their average dimensions (Fig. 3). The blanks were knapped by experimenter C. Lepers (TraceoLab) using direct hard-hammer percussion (sandstone). The backing was done with a hard hammer (sandstone) on a stone anvil to create a blunt, comfortable back for prehension, opposite a straight, unmodified cutting edge. All pieces measured between 2 and 4 cm in length and 1 to 2.5 cm in width. Their thickness ranged from 3 to 5 mm. The tools were manufactured from 4 different cores, all with a fine-grained structure from Velddrift, to minimise variation. Unfortunately, none of the silcrete cores was large enough to make all the experimental pieces. As we also had minimum dimensions to follow based on our reference archaeological sample, knapping was stopped when the core became too small to produce pieces with these dimensions. However, none of the cores was exhausted, and more lithics can be produced just with smaller dimensions. Following manufacture, all tools were systematically numbered and photographed with a Zeiss Axio Zoom V16 motorised microscope (magnification between ×6.5 to ×180– PlanApo Z0.5x/0.125 FWD 114 mm). This established a pre-use reference, facilitating the clear differentiation of use-wear from production-related features during later analysis. Tools were subsequently used, 15 as projectiles, 7 for other uses.

155

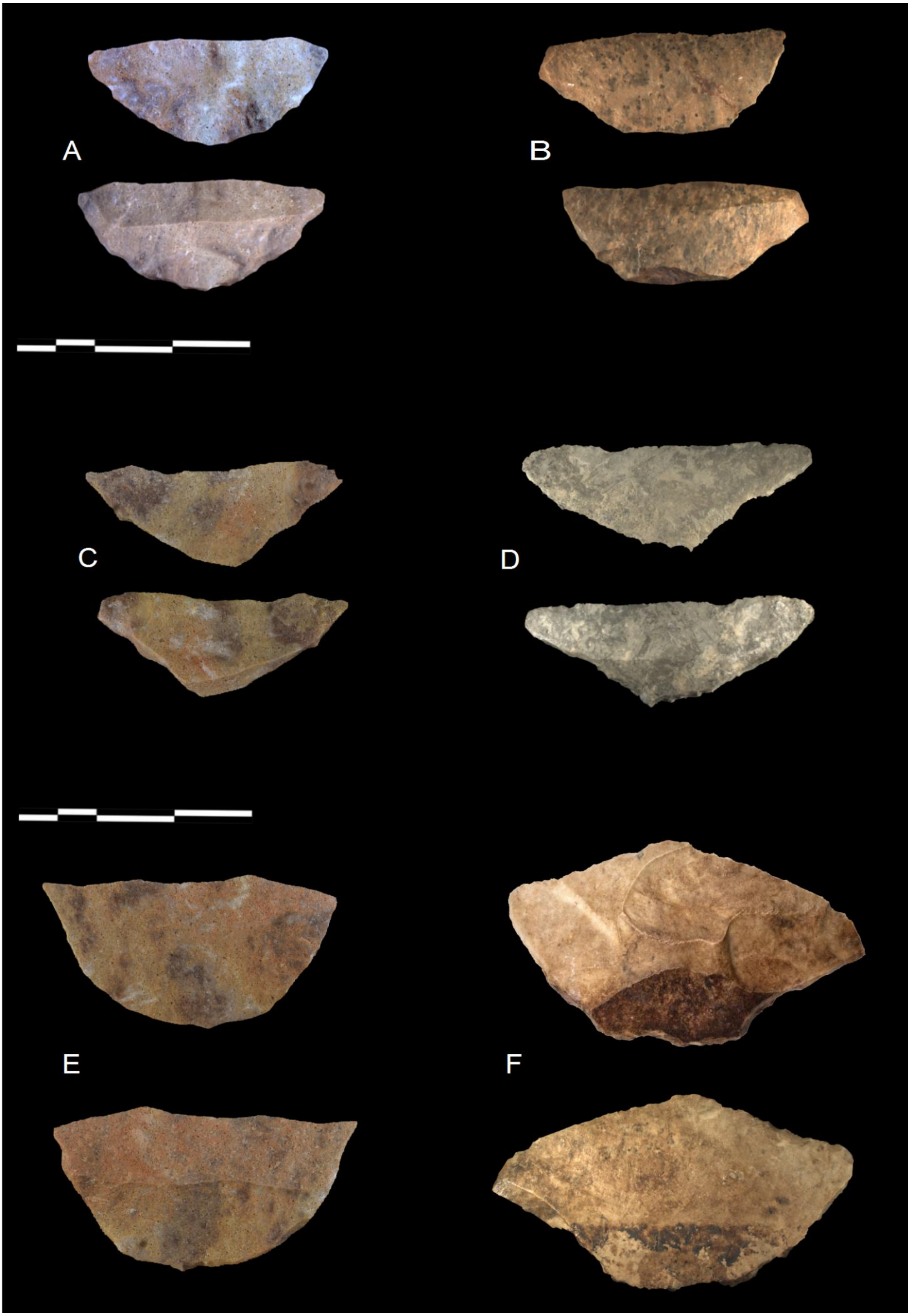

Fig. 3. This figure illustrates the experimental pieces A (EXP120/250), C (EXP120/263), E (EXP120/255) that were used in this experiment and the archaeological pieces B (DRS layer Fiona), D (DRS layer Kerry), F (DRS Ray/Ester) with similar morphology on which the morphology of the experimental pieces were based.

2.3 Projectiles

To best isolate and analyse damage from compressive force with a single propulsion mode, a thrusting action was chosen for the projectile experiment. This method generates exceptionally high compressive loads (Coppe et al., 2019), ensuring that the resulting use-wear traces are prominent and unambiguous.

2.3.1 Hafting positions

For this experiment, fifteen thrusting spears were assembled with a composite design: stone inserts were glued to a wooden fore shaft, which was then joined to the main wooden shaft via a split-joint secured with linen rope. We employed three hafting configurations (Fig. 4): 1) a lateral hafting arrangement with a single insert fitted into a groove along the side of the shaft, just behind the spear tip 2) a transverse tip, with a single insert hafted at the end of the fore shaft; 3) an oblique tip, with the insert set into the split in the shaft where the point was positioned in the centre. The retouched back of the insert was seated flush within this groove, and the angle of the retouched back determined the final angle of the insert relative to the shaft. The wooden spear point remained sharpened.

Fig. 4. Illustration of the three hafting arrangements used for the thrusting experiment: Lateral, Transversal and Oblique.

2.3.2 Adhesive

The stone inserts were secured to the fore shafts using a mastic composed of 70% pine resin and 30% harvested beeswax. This mixture was selected based on its proven efficacy in previous studies (Tydgadt and Rots, 2025, 2022) including the availability of a reference framework with flint projectiles that used the same glue. This glue mixture is quite mouldable and can form a smooth joint between the shaft and the lithic insert, which is critical for successful penetration without dehafting upon impact with the target's skin (Tydgadt and Rots, 2025). Its reliability made it suitable for the objective of this experiment, as it assured that the hafted-backed pieces would successfully enter the target and that possible impact fractures in the heat-treated silcrete would form.

2.3.3 Target

The target was constructed according to the protocols established by Coppe and Rots (Coppe and Rots, 2017). A deer skeleton, including the thoracic vertebrae, corresponding ribs, and clavicle, was reconstructed from fresh bone. The bones were cleaned by burying a carcass (with all organs and most meat removed) and leaving it to naturally decompose, allowing insects and bacteria to clean the bones. This is done because other cleaning methods, such as boiling, damage the bone structure and may affect the development of traces. After the bones were cleaned, they were suspended in the centre of a rectangular mould. The mould was then filled with ballistic gelatine. Once set, the gelatine block was demoulded and shaped to approximate the rough contours of a deer torso. Finally, a fresh deer hide was pulled taut over the target and secured to simulate the resistance and texture of a live animal. Using this setup instead of an animal carcass has several advantages; first, it is more stable throughout the experiment and makes lithic retrieval easier. Second, it also allows for a more economical use of the skeleton, which can, with this method, be reused with only the broken bones needing replacement. Finally, in some cases, lights and slow-motion cameras can be set up to capture the projectile's path through the gelatine.

2.3.4 Experimental Protocol

All spears were thrust by J. Coppe with a 7-meter run-up. They were used multiple times until clear macroscopic traces appeared or until hafting failed, defined as movement or detachment of the stone insert. For the laterally hafted configurations, if the organic point became too blunted while the barbs remained functional, it was resharpened to continue the experiment.

2.3.5 Cleaning Protocol

Following the experiment, the stone inserts were recovered. Any residual mastic was first removed using a heat gun. The heat gun was only used up until the point where the resin was melted enough to be wiped off, which is around 50°. Subsequently, the pieces were submerged in a 3% HCl solution for 5 min, rinsed, and placed in a weighing boat filled with distilled water and then placed in an ultrasonic bath for 10 minutes. The sequence was enough to remove all the residues from the projectile pieces. Acetone was used before using the metallographic microscope to ensure that all skin flakes and hand grease were removed.

2.3.6 Analytical Protocol

Macro- and microscopic analysis was conducted using a Zeiss V12 stereoscopic microscope (magnification ×8–×100) and a Zeiss Axio Zoom V16 motorised microscope (magnification ×6.5–×180). Fractures were documented and analysed according to the established criteria of (Coppe and Rots, 2025). An incident-light metallographic microscope (Zeiss AxioImager), with magnifications from 50× to 1000× and a set of six different objectives (EC Epiplan 5×/0.13 HD; EC EpiplanNeofluar 10×/0.25 HD DIC; LD EC Epiplan-Neofluar 20×/0.22 DIC; LD Epiplan 20×/0.40; LD Epiplan 50×/0.50; and LD EC Epiplan-Neofluar 100×/0.75 DIC) were used to analyse microscopic wear, particularly the possible presence of microscopic linear impact traces or more commonly known as “MILTs”” (Moss, 1983; Rots and Plisson, 2014).

2.4 Non-Projectile uses

For non-projectile activities, the aim was to create a broad reference library of use-wear traces on heat-treated silcrete, rather than to replicate specific prehistoric tasks. The Experimental tools were used for basic actions, including longitudinal, transverse, and engraving motions, on a variety of materials: dry hide, fresh wood, dry wood, dry bone, and ostrich eggshell (Table 1).

Table 1
Experimental details of the non-projectile tools.

Experimental number	Tool Type	Contact material	Movement	Action	Working angle	Total time used	Edge used
EXP120-25	Backed Flake	Dry hide	Bi-directional	Scraping	40-45°	45 Min	Unretouched cutting-edge
EXP120-16	Backed Flake	Ostrich eggshell	Bi-directional	Engraving	90°	45 Min	Unretouched cutting-edge
EXP120-43	Backed Flake	Dry Bone	Bi-directional	Sawing	90°	45 Min	Unretouched cutting-edge
EXP120-45	Backed Flake	Fresh Wood	Uni-directional	Shaving	30-35°	45 Min	Unretouched cutting-edge
EXP120-36	Backed Flake	Dry Bone	Uni-Directional	Scraping	40-45°	45 Min	Unretouched cutting-edge
EXP120-254	Backed Flake	Dry Wood	Bi-directional	Sawing	90°	45 Min	Unretouched cutting-edge
EXP120-251	Backed Flake	Fresh Wood	Bi-directional	Sawing	90°	45 Min	Unretouched cutting-edge

2.4.1 Experimental Protocol

For cutting dry wood, fresh wood, and dry bone, a sawing motion was used to create a groove. For scraping fresh wood, a unidirectional shaving motion (dragging the tool across the surface at a low angle towards the user's body) was used to remove the outer bark, with the tool's ventral surface in contact with the material. The same protocol was followed for scraping dry bone. For scraping dry hide, the same motion was applied to a piece of hide stretched on a frame, with the ventral surface held at a 40-45° angle. For the hide, however, a bidirectional motion was employed.

All tools were used for 20 minutes in their respective tasks, after which they were cleaned, photographed, and analysed for initial wear, which was also documented. Following this initial analysis, the tools were used for an additional 25 minutes, bringing the total time to 45 minutes. This duration was selected because previous experiments with silcrete indicated that distinguishable micro-wear traces only become apparent after approximately 30 minutes of use (Stephenson–Gordon, 2021).

2.4.2 Cleaning Protocol

All pieces were cleaned immediately after use, as it has been noted that residue removal is more effective before they have time to set (Asryan and Rots, 2024). The initial cleaning step for all pieces involved rinsing with distilled water to remove most particulate residues.

Subsequently, pieces used on bone were submerged in a 3% HCl solution for 5 min, rinsed, and placed in a weighing boat filled with distilled water in an ultrasonic tank for 10 min. The HCL solution was used for bone working as it dissolves calcium phosphate, effectively removing this type of residue. Pieces used on all other materials were submerged in a 1mol/L NaOH solution, rinsed and placed in a weighing boat in the ultrasonic bath for 10 minutes in distilled water. The NaOH solution was used for the rest of the uses, as it effectively removes hide-related residues by degrading fat and proteins and it also breaks down cellulose in plant residues. In most cases, a single 10-minute cycle in the ultrasonic tank was sufficient. If residues persisted, the ultrasonic treatment was extended in 5-minute increments until the tool was completely clean.

2.4.3 Analytical Protocol

Optical microscopy was performed using two microscopes. The first was a motorised stereo zoom microscope (Zeiss Axio Zoom V16) with objectives that provided magnification from 5.6× to 180×. The microwear analysis was primarily conducted under brightfield illumination. For this a motorised metallographic incident-light microscope (Zeiss AxioImager), which offered magnifications from 50× to 1000× using a set of six different (EC Epiplan 5×/0.13 HD; EC EpiplanNeofluar 10×/0.25 HD DIC; LD EC Epiplan-Neofluar 20×/0.22 DIC; LD Epiplan 20×/0.40; LD Epiplan 50×/0.50; and LD EC Epiplan-Neofluar 100×/0.75 DIC) was used. The photographs for this microscope were taken with a Zeiss Axio 503 colour camera mounted on a 60N-C 2/3" 0.63x adapter and using Zen Core software.

3. Results

3.1 Projectile

A total of fifteen spears, five for each of the three hafting configurations, were used. The majority of the spears successfully pierced the skin and penetrated the gelatine block. Initial difficulties were encountered with the sharpness of the organic points of spears with lateral insets (Table 2). These points were found to be insufficiently sharp and required resharpening before they could be used effectively. Furthermore, after each successful penetration, the organic points blunted significantly and required further resharpening for subsequent use, whereas the lateral stone barbs remained intact and functional. This differential wear is illustrated in Figure 5, which shows a spear after a single use with a visibly blunted organic point alongside an undamaged stone barb.

Table 2
General data about the result of the spear thrusting experiment.

Lithic number	Hafting arrangement	Number of successful attempts	Mode of failure	Mean Penetration depth (cm)	Number of unsuccessful attempts	Reason for unsuccessful attempts
246	Apical Oblique	2	Moved within the haft	48.5	0	
253	Apical Oblique	1	Dehafted	53.0	0	
261	Apical Oblique	1	Broken in haft	43.0	0	
262	Apical Oblique	1	Moved within the haft	22.0	0	
264	Apical Oblique	1	Moved within the haft	1.0	0	
247	Lateral barb	2	Organic point destroyed	15.5	2	organic point too blunt
248	Lateral barb	1	Broken in haft	6.0	1	organic point too blunt
252	Lateral barb	2	Moved within the glue	56.5	2	organic point too blunt
258	Lateral barb	1	Dehafted	47.0	0	
263	Lateral barb	3	Broken in haft	44.7	0	
250	Apical Transversal	1	Broken in haft	39.0	0	
255	Apical Transversal	1	Broken in haft	6.0	0	
256	Apical Transversal	2	Moved within the haft	32.5	0	
257	Apical Transversal	1	Dehafted	32.0	0	
259	Apical Transversal	2	Broken in haft	18.0	0	

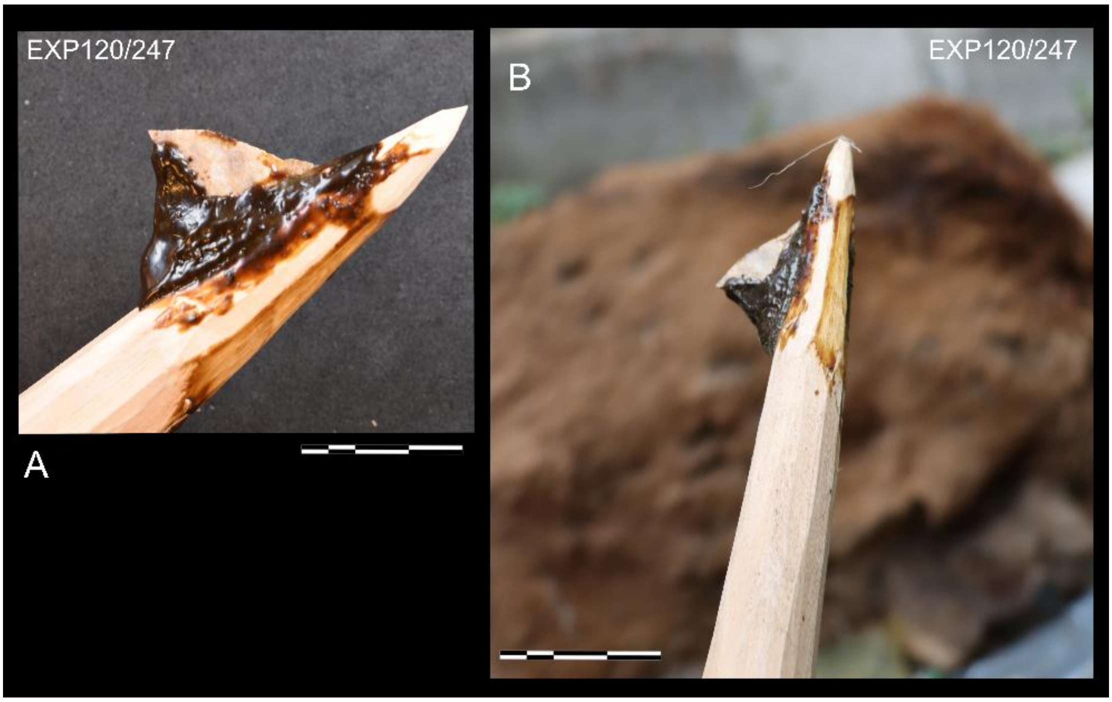

Fig. 5. Example of a spear with a lateral barb (A) before and (B) after an attempt, where the point was too blunt and rebounded on the skin

3.1.2 Projectile Experiments

The performance and durability varied significantly between the hafting configurations. The transversally hafted pieces penetrated to an average depth of 29.1 cm and could be used at most twice before catastrophic breakage occurred (Table 2).

The obliquely hafted pieces showed better penetration, with four out of five spears reaching an average depth of 43 cm. However, this setup was very prone to haft failure when contact was made with bone; all spear points dehafted on the first hit. Whether a projectile makes contact with bone can be observed thanks to the translucency of the target: after impact, the hide can be lifted and it is visible where the projectile entered and stopped. Also the sound during impact is very distinctive. Indeed, when the projectile hits bone, it makes a distinctly different sound than when it only pierces through gel. Finally, when the projectile is retrieved, there is some resistance and scraping against the bone, which again confirms the contact. .

Only one spear, which did not hit bone, was used twice (see Table 2).

For the laterally hafted spears, three of the five could be used more than once, with a mean penetration depth of 41 cm. As previously mentioned, the success of these spears was heavily dependent on the sharpness of the organic main point, which required frequent maintenance. However, with the sharpened organic point, all barbs penetrated successfully.

3.1.2 Use-Wear Traces

Macroscopic use-wear was most pronounced on specimens that had made contact with bone. Each fracture was assigned a point using the method proposed by Coppe and Rots (2025), even though this method was originally designed only for apical points made in flint. The projectile scoring method introduced by Coppe and Rots (2025) provides a framework for distinguishing projectiles based on impact traces related to compression from other types of use-wear. The system categorises macro-fractures into three distinct groups—bending breaks (BB), secondary damage (SD), and lateral scars (LS)—analysing the specific attributes of each to evaluate the degree of compression. Points are systematically added based on the presence or absence of specific diagnostic features (Table 3). By comparing the scores between projectile and non-projectile weapons, the researchers established a minimum "compression score" to eliminate ambiguity. Comparing experimental knives and projectiles, their data revealed a divide: knives never exceeded a compression score of 3. Consequently, the study concludes that any lithic artefact achieving a score higher than 3 can be confidently identified as having been used as a projectile (Coppe and Rots, 2025). In our experiment, 6 of the 15 used pieces scored 4 or higher (Table 4). Seven pieces scored below the threshold, and two displayed no wear at all.

Table 3
Points that are given to each fracture category based on its attributes (Adopted from Coppe & Rots 2025).

	Presence	Fissured termination (on ventral surface)	Length 1.5 times longer than the thickness of the cross-section of the fracture initiation	Multiple	Initiation is absent	Initiation on the abrupt termination of a preceding fracture	Direction opposite to the primary fracture orientation	Abraded initiation	Maximum value per fracture
BB	+1	+1	+1	/	/	/	/		3
SD	+1	+1	/	+1	+1	+1	/		5
LS	+1	+1	/	+1	+1	/	-1	-1	4

Table 4
Fracture descriptions for the pieces used in the spear thrusting experiments, including the compression score points (according to Coppe & Rots, 2025)

Piece	Fracture ID	Initiation Morphology	Location of Initiation	Orientation	Location of Termination	Termination	Composition	Fracture Type	Category	Fissure	Score	Total
248	248_1	Bending	Dorsal	Apex to base	Ventral	Step	Single	Break	Bending break	No	2	2
248	248_2	Absent	Termination of Previous Scar	Apex to base	Ventral	Step	Single	Scar	Secondary damage	No	0	
250	250_1	Absent	Ventral	Apex to base	Dorsal	Step	Multiple	Scar	Lateral scar	Yes	4	7
250	250_2	Absent	Dorsal	Perpendicular	Ventral	Step	Multiple	Scar	Lateral scar	No	4-1	
252	252_1	Absent	Ventral	Apex to base	Dorsal	Step	Multiple	Scar	Lateral scar	Yes	4	8
252	252_2	Absent	Dorsal	Apex to base	Ventral	Step	Multiple	Scar	Lateral scar	Yes	4	
253	253_1	Bending	Ventral	Perpendicular	Dorsal	Step	Single	Scar	Lateral scar	No	0	0
253	253_2	Bending	Ventral	Perpendicular	Dorsal	Feather	Multiple	Scar	Lateral scar	No	0	
247	247_1	Bending	Back	Apex to base	Cutting Edge	Snap	Single	Break	Bending break	No	0	0
255	255_1	Bending	Dorsal	Apex to base	Ventral	Step; hinge	Single	Break	Bending break	Yes	3	5
255	255_2	Missing	Dorsal	Apex to base	Ventral	Step	Single	Scar	Lateral scar	No	2	
256	256_1	Bending	Ventral	Perpendicular	Dorsal	Step	Single	Scar	Lateral scar	No	1	1
257	257_1	Absent; cone	Dorsal	Apex to base	Ventral	Step	Multiple	Scar	Lateral scar	Yes	4	4
258	258_1	Absnet; Cone	Ventral	Apex to base	Dorsal	Step	Multiple	Scar	Lateral scar	Yes	4	8
258	258_2	Absent	Ventral	Apex to base	Dorsal	Hinge	Multiple	Scar	Lateral scar	Yes	4	
259	259_1	Bending	Ventral	Apex to base	Ventral	Step; feather	Multiple	Scar	Lateral scar	No	2	2
259	259_2	Bending	Dorsal	Perpendicular	Ventral	Step	Single	Scar	Lateral scar	No	0	
261	261_1	Absent; cone	Dorsal	Perpendicular	Ventral	Step	Multiple	Scar	Lateral scar	Yes	0	0
261	261_2	Bending	Dorsal	Apex to base	Back	Snap	Single	Break	Bending break	No	0	
262	262_1	Absent	Dorsal	Apex to base	Ventral	Step; hinge	Multiple	Scar	Lateral scar	Yes	4	4
262	262_2	Missing	Ventral	Perpendicular	Ventral	Step	Multiple	Scar	Lateral scar	No	0	
263	263_1	Bending	Dorsal		Ventral	Snap	Single	Break	Bending break	No	0	0
263	263_2	Bending	Ventral		Dorsal	Snap	Single	Break	Bending break	No	0	
263	263_3	Bending	Ventral		Dorsal	Snap	Single	Break	Bending break	No	0	

The five transversally hafted pieces had an average compression score of 3.8, with three exceeding a score of 4. For this category, however, the point system needed to be adapted. In the original Coppe and Rots (2025) method, a lateral scar is counted only if it is oblique to the tool's axis—typically at the apex. For the transversal pieces, all scars were perpendicular to the long axis due to the hafting orientation. Therefore, the axis was redefined: the cutting edge was treated as the apex and the base as the back, allowing all lateral scars oriented from apex to base to be counted (Fig. 6). This adjustment was necessary because the original method was developed for apically hafted points, whereas these pieces were hafted transversally.

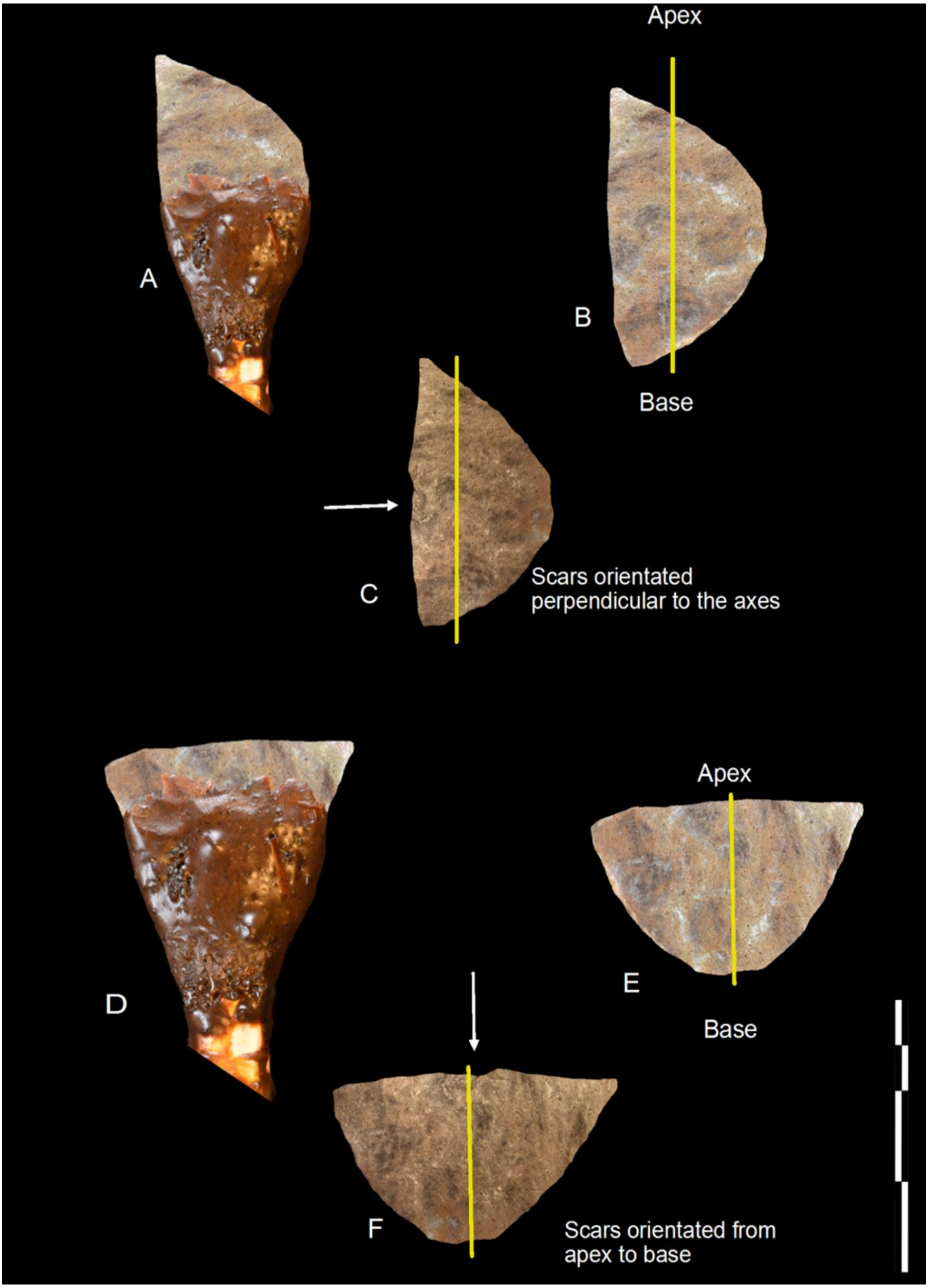

Fig. 6. This figure shows the orientation of the lateral scars in relation to the hafting axis **with the white arrows indicating the directionality of the scars**. (A) depicts an apical axially hafted piece. (B) indicates the locations of the apex and base, as well as the axes, assuming the piece is hafted in this manner. (C) illustrates the orientation of the use-wear scars, which run parallel to the axis defined in b based on the apex and base positions. (D) shows the same piece hafted apically and transversely, with (E) indicating the apex and base locations in this alternative hafting

scenario. In this configuration, as seen in (F), the use-wear scars would run from the apex to the base rather than parallel to the axis.

The obliquely hafted pieces were more comparable to those in the Coppe and Rots (2025) experiment, and no axis adjustment was made. However, this category had the lowest average compression score (1.3), and only one of the five pieces met the threshold. This can be attributed to two factors: first, two of the obliquely hafted pieces showed no wear; second, although the other pieces exhibited wear, the lateral scars did not register the expected orientation, likely due to raw material properties. The scars appeared perpendicular and thus could not be counted. The laterally hafted pieces had an average score of 3. Two of the five pieces scored high enough to meet the threshold; these pieces displayed clearly oriented scars with fissurations and frequently lacked initiations.

Although 40% of the pieces in this experiment scored above the projectile threshold, the overall mean remains low compared to that of the Coppe and Rots (2025) study. In their experiment, the small, backed pieces—the closest in length to those in our study—had an average score of 3.4, with a maximum of 12. Our transversal category slightly exceeded this average, but only after the axis adjustment was applied. Additionally, some laterally hafted pieces achieved a score of 8, the highest in our experiment. These findings highlight the value of expanding this method to include other raw materials and hafting orientations to capture the full diagnostic pattern for projectile identification.

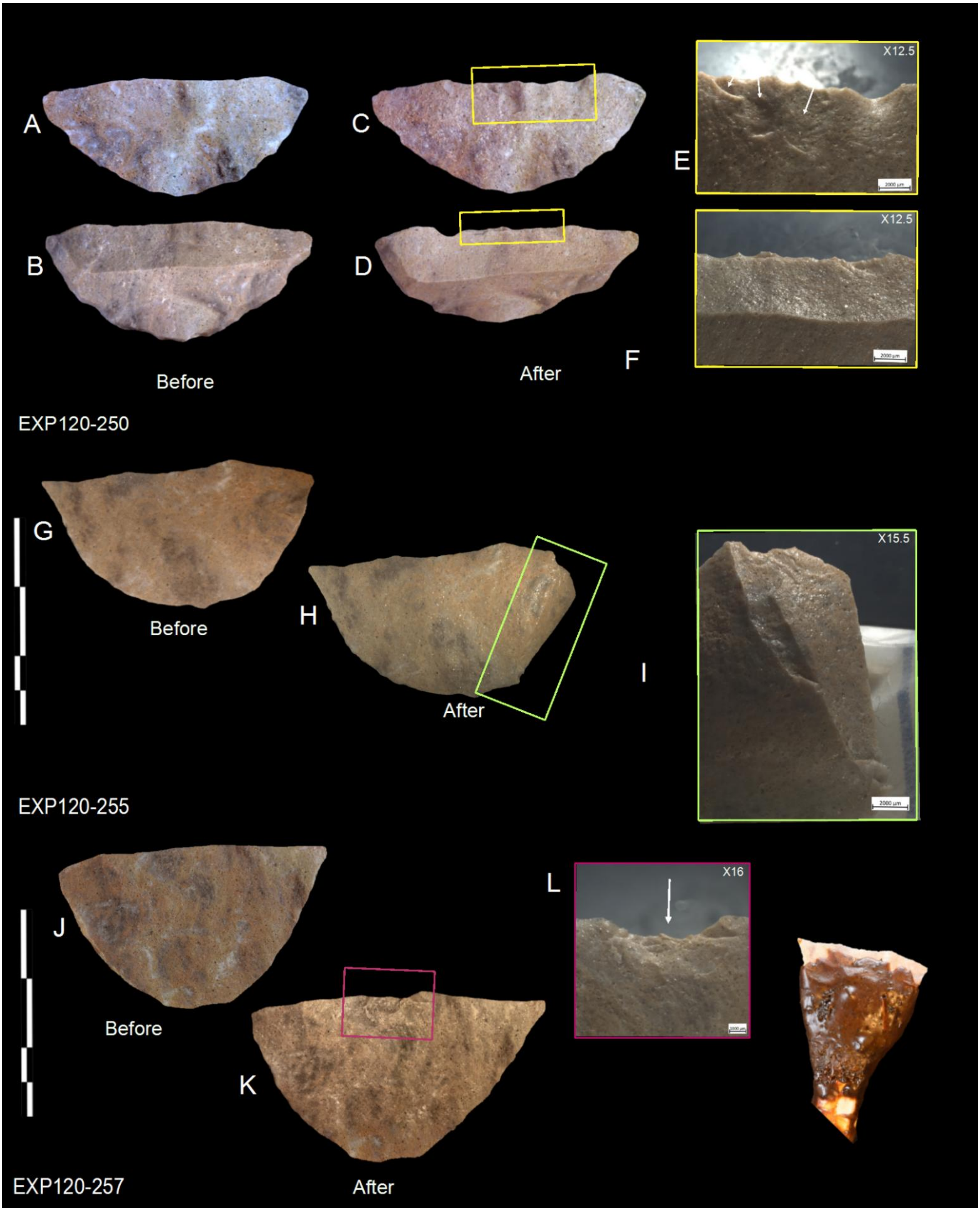

Fig. 7. Damage traces on pieces hafted transversally with white arrows indicating the directionality of the scars. For the first piece (120-250), images (A) and (B) show its ventral and dorsal surfaces before use, while (C) and (D) show the same surfaces after use. Detailed views of the post-use damage are provided, with image (E) showing lateral scars propagating onto the ventral surface terminating in steps and image (F) showing lateral scars propagating onto the dorsal surface. For a second piece (120-255), images (G) and (H) contrast the ventral surface before and after use. A macro photograph (I) details the resulting damage, showing a bending break alongside a lateral scar, both terminating in steps. For a third piece (120-257), images (J) and (K) show its ventral surface before and after use. A

final macro photograph (L) showcases the damage, characterised by crushing and multiple lateral scars that have propagated onto the ventral surface.

With the adjustments, the points system could thus be applied. The damage observed on heat-treated silcrete could also be described using existing terminology originally developed for flint. Transversally hafted pieces had scars with missing initiations, abrupt terminations, and fissuring at the termination (Fig. 7). All five of the transversally hafted pieces penetrated the target, and two of the 5 could be used a second time. Only one did not exhibit distinct use wear traces. EXP 120/256, although it was used twice with a mean penetration depth of 32 cm, exhibited only one small bending-initiated scar propagating onto the dorsal edge. The overall mean penetration depth for the transverse pieces was 25.5 cm.

Two of the five obliquely hafted pieces (EXP120/246 and EXP120/264) displayed no macroscopic wear, probably due to an absence of contact with bone. The projectile from test EXP120/264 dehafted prematurely upon penetrating the first centimetre of the skin and gelatine composite. This early failure is the probable reason for the lack of diagnostic traces. Two of the remaining three pieces exhibited distinct wear: one had a bending fracture and lateral scars at the base; the second, which impacted the clavicle, also had multiple lateral scars at the base with intense fissurations (Fig. 8). The third piece exhibited multiple bending-initiated scars originating in the medial section. These propagated onto the dorsal surface, terminating in feather features, while smaller lateral scars extended from the medial area toward the base.

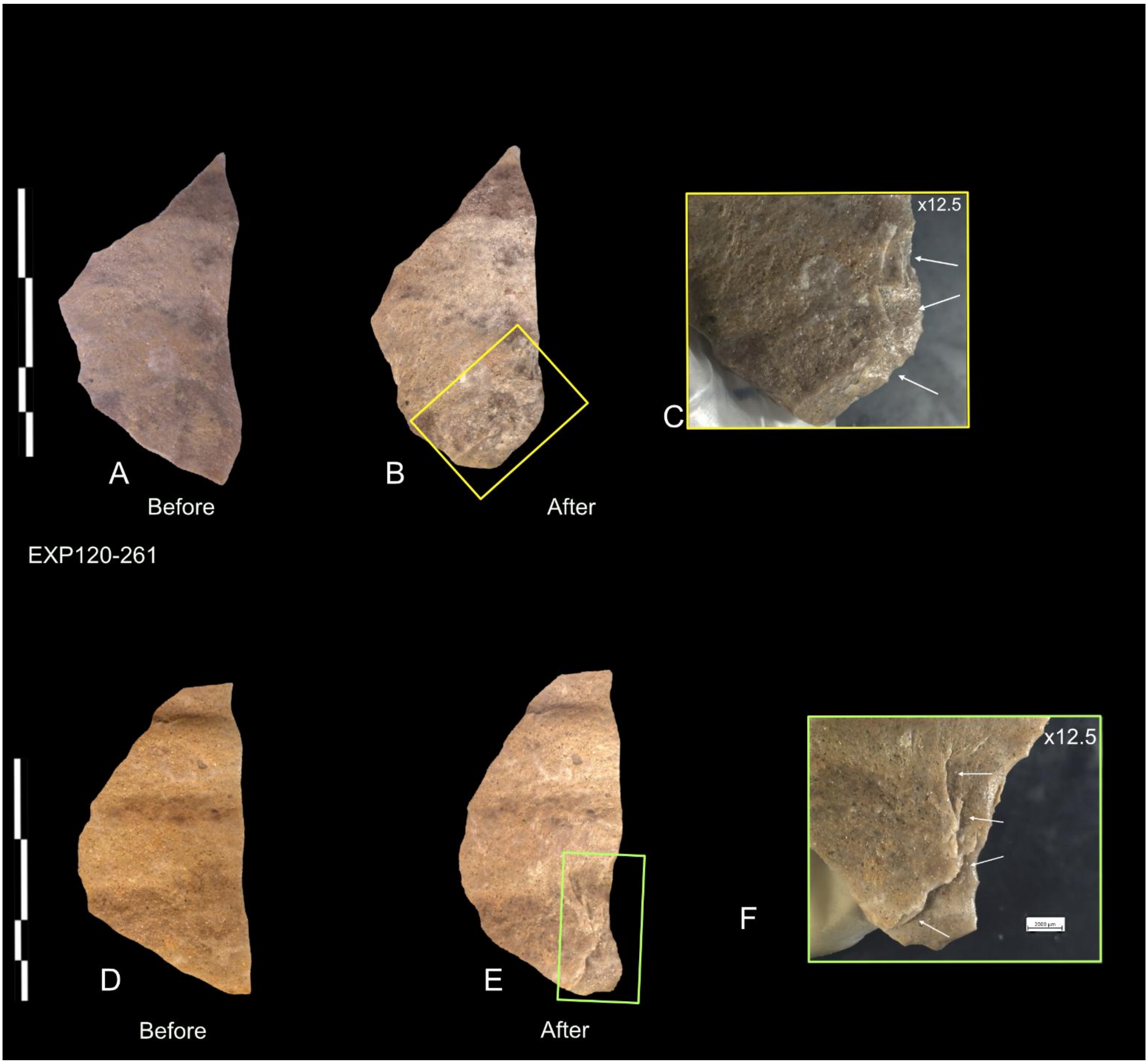

Fig. 8. Examples of pieces that were hafted obliquely with the white arrows indicating the directionality of the scars. Images (A) and (B) show the ventral face of tool 120-261 before use and after use, where a bending break and lateral scars have propagated onto the ventral surface. A zoomed-in photograph at 12.5x magnification (C) provides a detailed view of this bending break and the lateral scars. For a second piece, images (D) and (E) show the ventral face of tool 120-262 before use and after use, with the latter displaying prominent lateral scars. A corresponding 12.5x macro photograph (F) shows these lateral scars propagating onto the ventral surface in detail, showing their hinge terminations and associated fissurations.

Among the laterally hafted pieces (barbs), three exhibited lateral scars. These scars were obliquely oriented and showed some fissurations at their terminations. One barb broke into multiple pieces upon impact (Fig. 9), and another had a scar at the apex ending in a step fracture with secondary damage (Fig. 10). Some pieces had lateral scars (EXP120/258, Fig. 10) that were uniformly oriented. In other cases (e.g., EXP120/252, Fig. 10), the scars formed two opposing sets of orientations, likely due to the retrieval of the point, which caused opposing scars. Importantly, none of the projectile pieces showed observable MLITs under a metallurgical microscope.

Fig. 9. A photograph of the before and after of the experimental piece EXP120/263 showing 2 bending breaks that occurred during usage.

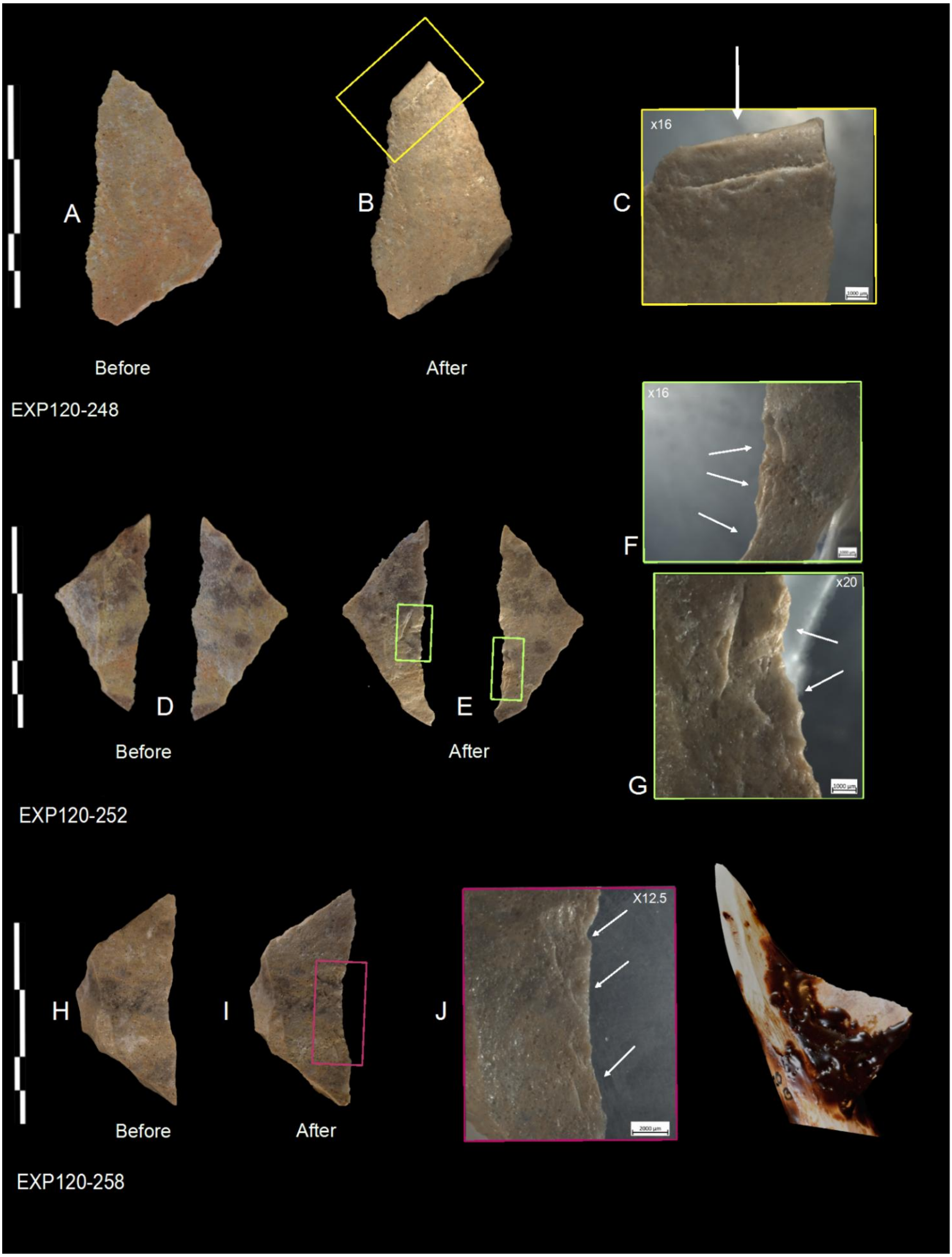

Fig. 10. Summary of the distinct use-wear traces identified on the lateral barbs including white arrows showing the directionality of the scars. Images A and B show the ventral surface of Piece 120-248 before and after use, respectively, while a macro photograph (C) details a bending break that has propagated onto the ventral surface and terminated in a step. For Piece 120-252, image D shows its dorsal and ventral surfaces before use, and image E shows them after use. A detailed view (F) reveals multiple lateral scars that have propagated onto the ventral surface and terminated in steps. A corresponding feature (G) shows a lateral scar terminating in a step on the dorsal surface. Finally, images H and I show the dorsal surface of Piece 120-258 before and after use, with a detailed view (J) highlighting obliquely orientated lateral scars that have propagated onto the dorsal surface.

3.2 Non-Projectile Experiments

The tools in this phase of the experiment were used on various contact materials in transversal and longitudinal directions. The development of edge damage on these silcrete tools shows a vital shift from quick deterioration to stable edges. Due to the initial breakage, the tools' efficiency dropped during the first 35-40 minutes when used on hard materials such as dry wood and bone. This is directly linked to an intense initial period of micro-fracturing, where the sharp edge experienced continuous and significant loss, as depicted in Figure 11. This phase is characterised by the removal of fragile, high points on the edge through small, brittle fractures.

Table 5
Summary of the use-wear types for different actions after 20 and 45 min of use.

Artefact	Use	Material	Duration	Edge rounding	Edge rounding distribution	Polish development	Polish distribution	Polish texture	Striations
EXP120/16	Engraving	Eggshell	20 min	Light	High points	Absent	Absent	Absent	Absent
EXP120/16	Engraving	Eggshell	40 min	Moderate	High points	Absent	Absent	Absent	Absent
EXP120/25	Scraping	Hide	20 min	Moderate	High points	Light	Band on edge	Rough	Absent
EXP120/25	Scraping	Hide	40 min	Heavy	Continuous	Moderate	Band along the edge	Rough/pitted	Absent
EXP120/26	Cutting	Dry wood	20 min	Absent	Absent	Absent	Absent	Absent	Absent
EXP120/26	Cutting	Dry wood	40 min	Moderate	High points	Moderate	Isolated spots	Smooth	Isolated; Parallel
EXP120/36	Scraping	Bone	20 min	Light	High points	Absent	Absent	Absent	Absent
EXP120/36	Scraping	Bone	40 min	Light	High points	Absent	Absent	Absent	Absent
EXP120/251	Cutting	Fresh wood	20 min	Light	High points	Light	Isolated spots	Smooth	Isolated; Parallel
EXP120/251	Cutting	Fresh wood	40 min	Light	High points	Moderate	Isolated spots	Smooth with pits	Isolated; Parallel
EXP120/254	Shaving	Fresh wood	20 min	Light	High points	Light	Isolated spots	Smooth	Absent
EXP120/254	Shaving	Fresh wood	40 min	Light	High points	Light	Isolated spots	Smooth	Absent
EXP120/260	Cutting	Bone	20 min	Absent	Absent	Absent	Absent	Absent	Absent
EXP120/260	Cutting	Bone	40 min	Moderate	High points	Moderate	Isolated spots	Rough	Absent

Table 6
Summary of the edge removals for different actions after 20 and 45 min of use.

Artefact	Use	Material	Duration	Edge removals	Initiations	Terminations
EXP120/16	Engraving	Eggshell	20 min	Absent	Absent	feather
EXP120/16	Engraving	Eggshell	40 min	Isolated	Bending; Missing	Feather
EXP120/25	Scraping	Hide	20 min	Isolated	Bending	-
EXP120/25	Scraping	Hide	40 min	Absent	Absent	-
EXP120/26	Cutting	Dry wood	20 min	Close together	Cone; Bending	Mix
EXP120/26	Cutting	Dry wood	40 min	Close together	Cone; Bending; Missing	Mix
EXP120/36	Scraping	Bone	20 min	Scalar	Cone; Missing	Feather

EXP120/36	Scraping	Bone	40 min	Scalar	Missing	Feather
EXP120/251	Cutting	Fresh wood	20 min	Isolated	Bending	Feather
EXP120/251	Cutting	Fresh wood	40 min	Isolated	Bending	Feather
EXP120/254	Shaving	Fresh wood	20 min	Isolated	Bending	Feather
EXP120/254	Shaving	Fresh wood	40 min	Close together	Bending	Feather
EXP120/260	Cutting	Bone	20 min	Close together	Cone; Bending	Mix
EXP120/260	Cutting	Bone	40 min	Close together	Cone; Bending; Missing	Mix

After the first 20 minutes, the edge stabilised. The previously sharp, fragile edge became more durable and rounded, reducing the risk of sudden failure. As shown in Figure 11, although the scars from the initial phase were still visible after 45 minutes of use, they started to wear down and became more rounded in appearance. This marks a fundamental shift in the dominant wear process: after the initial break-in period, the wear mechanism transitions from macro-scale fracturing to micro-scale abrasion, allowing the gradual development of classic use-wear traces such as striations, polish, and edge rounding.

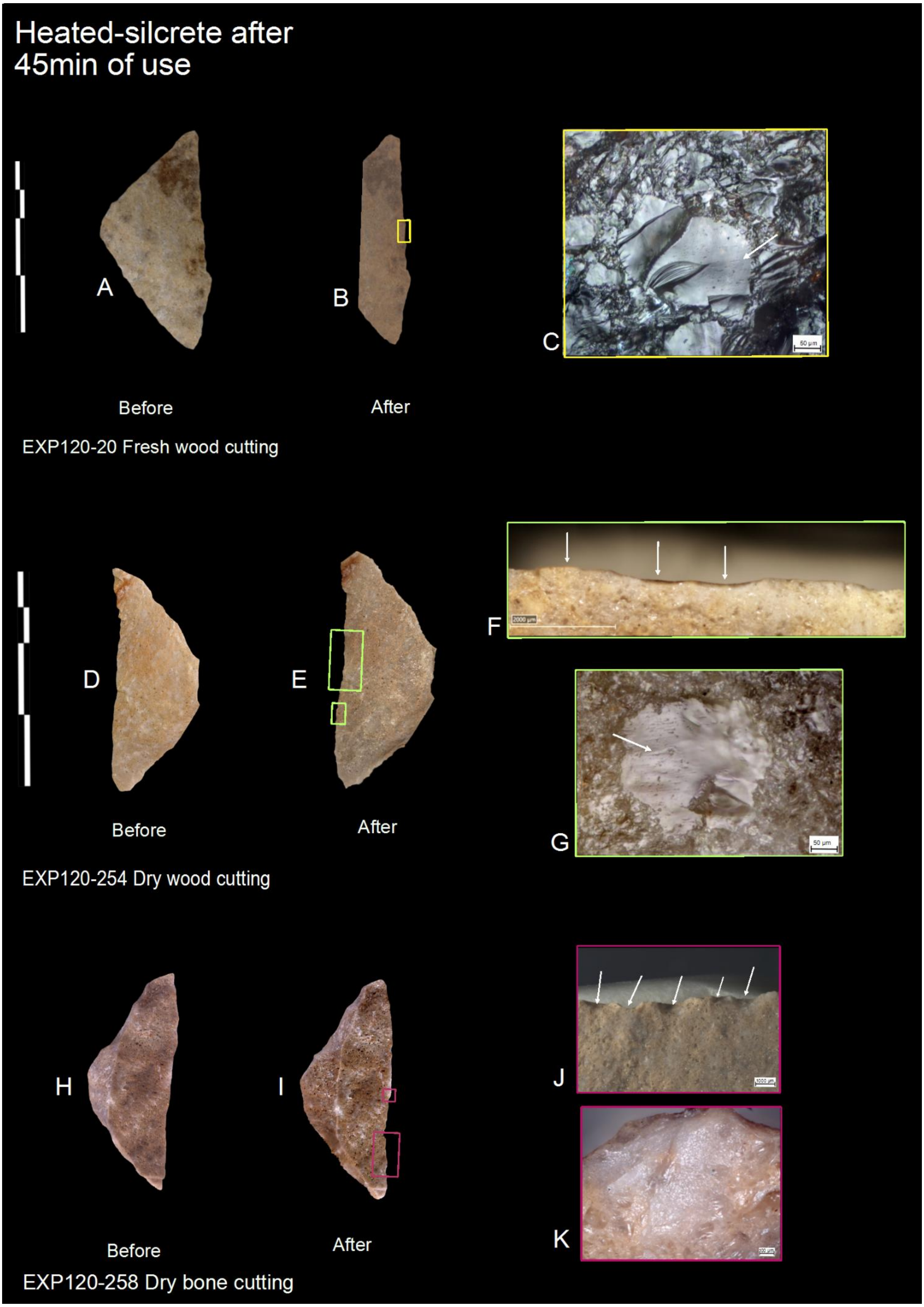

Fig. 11. Here, the wear patterns on stone tools after use on different materials are illustrated. Images (A) and (B) show the ventral surface of tool 120-20 before and after 45 minutes of cutting fresh wood, respectively, and C shows short striations on its quartz crystals. For dry wood cutting, images (D) and (E) depict the ventral surface of tool 120-

254 before use, and after use, (F) also shows the ventral surface with bending-initiated scars indicated by the white arrows and on (G), short striations are visible indicated by the white arrow. Finally, images (H), (I), and (J) focus on the dorsal surface of tool 120-258, used for cutting dry bone. The "after use" images (J) show how cone-initiated scars, indicated by the white arrows,have propagated onto the dorsal surface, creating a jagged edge, accompanied by (K) a rough polish on the higher areas.

Cutting Activities: The tools used for cutting wood displayed densely grouped, close-to-the-edge scarring. The scars predominantly featured feather terminations and diffuse or missing initiations. The pieces used on fresh wood had very sparse scars, while the piece used to cut dry wood had notably more scars along the edge (Fig. 11). In stark contrast, the cutting tool showed much more obvious damage. The scars were more invasive (travelling further from the edge) and had abrupt terminations, creating a jagged, crushed edge. This is a direct result of bone's extreme hardness and resistance, which cause more destructive, brittle fractures upon contact (Fig. 11).

Striations were observed exclusively on cutting tools; they were found only on the quartz crystals embedded within the matrix. Their short, discontinuous nature is a direct result of this composite structure. The matrix wore down more readily, leaving the quartz crystals protruding slightly. Any linear motion, such as the longitudinal action parallel to the cutting edge observed during woodcutting, would cause abrasive particles to score the quartz. However, this process was constantly interrupted as the scoring agent moved from the high point of a quartz crystal down into the adjacent, lower-lying silcrete matrix, preventing the formation of long, continuous striations. This is why such features were recorded only on quartz and were consistently short. This phenomenon was observed on both fresh and dry wood-cutting tools, as shown in Figure 11. Edge rounding was observed exclusively on the high points of all cutting tools after 40 minutes of use. At the 20-minute mark, only the tool used to cut fresh wood showed edge rounding of the protruding surface topography. In contrast, edge rounding was not observed on tools used for cutting bone or dry wood after 20 minutes, probably because edge breakage occurred too rapidly for edge rounding to develop. Polish followed a similar pattern. It developed most rapidly on the tool used for cutting fresh wood: light, isolated polish was visible after only 20 minutes, and by 40 minutes, moderate polish was present on isolated spots exclusively on quartz crystals. For tools used to cut dry wood and bone, polish developed only in isolated spots after 40 minutes. Notably, the bone-cutting tool showed rough polish in isolated areas at this stage (Fig. 11).

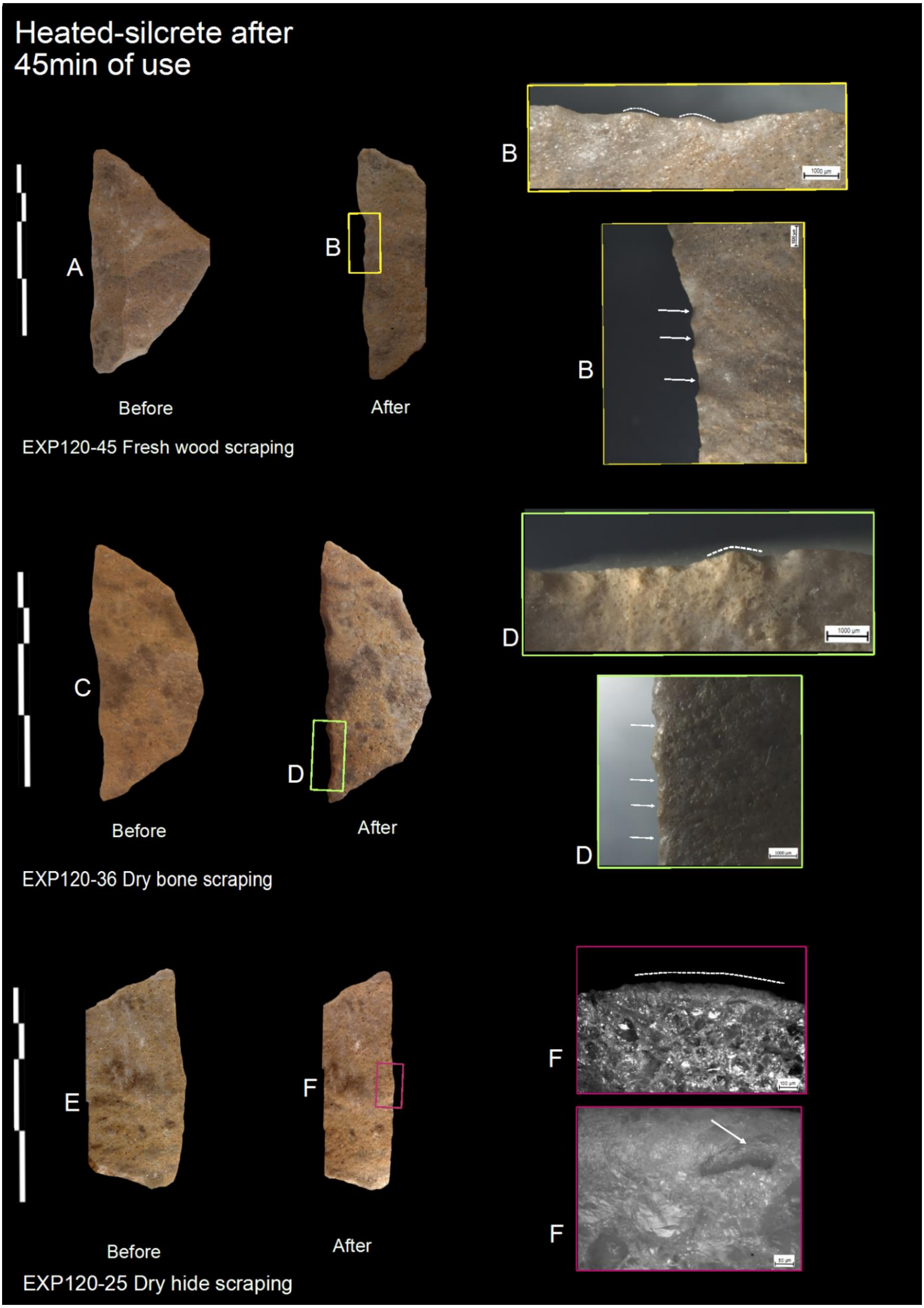

Fig. 12. Here the wear patterns developed from scraping different materials are shown. Images (A) and (B) show the dorsal surface of tool 120-45 before use and after 45 minutes of scraping fresh wood, with the latter exhibiting

both edge rounding and bending-initiated scars, indicated by the white arrows, that have propagated onto the dorsal surface. For bone scraping, images (C) and (D) contrast the ventral surface of Piece 120-36 before use and after 45 minutes of use, (D) also depicting edge rounding and the formation of small bending scars, indicated by the white arrows. Finally, images (E) and (F) illustrate the ventral surface of Tool 120-25 before and after 45 minutes of hide scraping, which resulted in intense edge rounding and a developed polish, indicated by the white arrow, along the working edge.

Scraping Activities: The scraping motion was performed with the unretouched, sharp edge, while holding the backed portion in the hand. This places the entire edge under consistent pressure, which produced a distinct scar pattern characterised by bending initiations (where the force pushes the edge back before a flake detaches) and feather terminations.

On bone, this action was performed unidirectionally and was particularly destructive. The scars were continuous, highly invasive, and often removed the contact edge completely, leading to rapid and severe blunting (Fig. 12).

Scraping fresh wood was also performed unidirectionally and produced a less severe version; the scars were fewer, less invasive, and concentrated in the middle of the tool where contact pressure was highest (Fig. 12).

Hide scraping was performed bidirectionally, resulting in very few, mostly isolated scars. The pliable nature of hide reduces direct mechanical stress on the edge, resulting in minimal fracturing, with the primary wear consisting of abrasive edge rounding and polish (Fig. 12).

Most tools performed well over the 45 min use period. In low-abrasion tasks like cutting, the edge remained relatively_intact for the first 20 minutes. However, after 45 minutes of use, all cutting tools showed blunting. High-abrasion tasks like dry hide scraping, which involve dragging the tool across a tightly stretched skin, induced immediate and noticeable wear. Clear edge rounding was apparent after just 20 minutes, escalating to heavy edge rounding after 45 minutes._For other scraping tasks on fresh wood and dry bone, some edge rounding became noticeable only after 45 minutes, as the edge stabilised: the most fragile high points were worn down first, creating a more durable, albeit rounded, working surface. The bone-scraping tool became ineffective after 30-35 min of use, as the edge was almost completely worn down. No striations were observed on any of the scraping or shaving tools. Bone scraping also produced no polish, even after 40 minutes. In contrast, hide scraping developed a light band of polish along the edge after 20 minutes, which progressed to a moderate band after 40 minutes of use. Shaving fresh wood yielded a light, smooth polish after 20 minutes, which remained consistent and did not intensify further after 40 minutes.

Engraving Activity: The tool used on ostrich eggshell presented a unique case. It experienced considerable edge loss, but not through the formation of clear, conchoidal scars. Instead, the edge underwent a process of crumbling, in which the edge disintegrated under the highly localised, pinpoint pressure required for engraving. This resulted in a general degradation of the edge without the formation of distinct, isolated flake scars. The ostrich eggshell engraving tool exhibited minimal wear initially but developed light to moderate edge rounding over time—distinct from the smooth edge rounding observed on the hide scraping tool—reflecting the hard, abrasive nature of the eggshell. No polish or striations were observed on this tool

4. Discussion

This study shows that heat-treated silcrete exhibits broad macroscopic wear patterns similar to those of more uniform materials like flint. However, its distinct internal structure causes notable differences at both macro- and microscopic levels, requiring a customised approach for wear analysis. On a macro scale, edge damage patterns generally follow established principles from flint research. The hardness of the material influences fracture types: contact with hard substances often leads to cone-shaped fractures and sudden breakages, typical of brittle, high-impact reactions.

While working with softer materials generates more bending fractures, resulting from a more pliable form of contact. Similarly, the motion of scraping reliably creates unifacial scarring, and when applied to pliable materials like hide, it leads to pronounced edge rounding as the worked material conforms to and abrades the tool's contour. In the context of projectile use, the fracture attributes traditionally used (Coppe and Rots, 2017) are appropriate for describing fractures in silcrete. Heat-treated silcrete also exhibits classic features of high-velocity impact, such as fissures and abrupt terminations resulting from intense compression forces.

However, the critical distinction lies in the inherent heterogeneity of silcrete, which significantly complicates its analysis. The complex composite structure of quartz crystals embedded in a softer matrix makes it difficult to interpret individual scars. Unlike flint tools, which tend to show clear, predictable fracture patterns, scars on silcrete often have their initiation, path, and orientation influenced by the stone's internal grain. A fracture may initiate on a quartz crystal but terminate abruptly upon hitting the matrix or be redirected along crystal boundaries. This makes the standard "reading" of fracture initiation and orientation, a cornerstone of projectile analysis, notably more challenging on heat-treated silcrete.

This challenge is compounded at the microscopic level. Firstly, the naturally shiny and irregular surface of silcrete creates visual noise, making the initial identification of subtle polishes and striations more difficult than on the smoother, more homogeneous surfaces of obsidian or flint. Secondly, and more fundamentally, the development and appearance of micro-wear are distinctly different. There appears to be a delayed onset of polish and edge rounding. This is because the initial use-phase is dominated by micro-fracturing and edge stabilisation; only once a stable edge geometry is achieved do the classic abrasive and polish-forming processes begin to dominate.

Furthermore, the resulting polish and striations do not resemble those of flint. Instead of forming a continuous, cohesive polishing across the tool surface, microwear on silcrete is localised and isolated more in line with quartzite (Ollé et al., 2016). Other studies have also noted that striations and polish do not form as readily on quartzite as on homogeneous material (Liu and Chen, 2016). Other studies on quartzite, however, have found both striations to be present and useful in determining the hardness of the worked material (Lemorini et al., 2014). Pedergnana and Olle (2017) found that through SEM imaging and sequential experiments, striations of quartz grains in the quartzite appear after a time and then disappear again after further use due to continuous friction ~~(Pedergnana and Ollé, 2017)~~. More in-depth studies and a larger sample are needed to determine whether heated silcrete follows the same pattern. In our experiment, polish and, notably, striations primarily developed on exposed quartz crystals, which are the highest points in the micro-topography. This explains why striations are usually short and discontinuous; they only form on these isolated crystal "islands" and cannot extend across the lower matrix. Because the stone is composite, the quartz crystals and the matrix respond differently to friction, hindering the development of large, uniform polished areas typical of homogeneous flint.

The findings of this study are broadly consistent with previous research on silcrete, although those earlier studies were conducted exclusively on unheated material. Use-wear was observed to develop more slowly on unheated silcrete than on homogeneous materials such as flint (Stephenson–Gordon, 2021), porcelain, and glass (Munt et al., 2023). On our experimental tools, polish formation after 20 minutes was light or absent, regardless of contact material or action, and tended to develop primarily on high-topography areas. This aligns with Stephenson’s (2021) observation that polish formed very gradually—only 20% of tools exhibited any polish after 30 minutes of use, increasing to 70% after 60 minutes. Hilbert (Hilbert et al., 2022), also reported polish forming on elevated areas; however, in their case, it developed within five minutes. This discrepancy is likely due to their contact material (sandstone), which produced a distinct mineralogical polish.

Although polish seems to form most readily on high-topographic areas, both our study and that of Munt et al. (2023) found that hide-working produced polish on high points and in valleys. In both cases, the hide-working polish was also described as rough.

Regarding edge rounding, Stephenson (2021) similarly found, consistent with the current study, that edge rounding occurred rapidly, particularly when working with softer materials. On our heat-treated silcrete, we observed the same phenomenon: the pieces fragmented more easily on harder materials, which reduces prolonged contact and results in slower edge rounding development.

In our experiments, striations were most clearly visible on woodworking tools, a pattern also identified by Munt et al. (2023). Conversely, Stephenson (2021) reported seeing striations on scraping tools and bone-cutting implements, which we did not observe. This difference might be due to the excessive fracturing of heat-treated silcrete in our study, potentially preventing striation formation. Alternatively, increasing experimental duration, expanding the sample size to improve the chances of detecting such features, or employing SEM analysis for more detailed surface examination could be necessary.

5. Conclusion

In summary, while use-wear on heat-treated silcrete follows the general "language" of traceology established for other stones, it speaks with a unique "accent" dictated by its heterogeneous structure. The results of this study concur with previous research on other coarse-grained materials, confirming that interpretable wear requires extended use (over 30 minutes), that striations form primarily on exposed quartz crystal surfaces, and that while some macroscopic patterns are comparable to flint, the microscopic picture is markedly more complex.

This complexity arises directly from the material's composite nature. At a macroscopic scale, fracture paths are irregularly determined by the internal grain, challenging standard interpretations of initiation and termination. Microscopically, the delayed onset of polish, its isolated development on quartz grains, and the short, discontinuous nature of striations that cannot traverse the softer matrix all represent fundamental divergences from the cohesive wear patterns seen on homogeneous materials like flint or obsidian.

Therefore, this study represents a foundational yet preliminary step towards building a robust reference collection for heat-treated silcrete. A larger sample size and more extensive experimentation across a wider range of contact materials and motions are required to fully decipher its complex micro-wear signatures and establish diagnostic criteria. The ultimate goal is to move beyond assumptions based on flint models and build a reliable, material-specific interpretive framework. This will enable more accurate functional identification of heat-treated silcrete tools, thereby refining our understanding of technological behaviours related to assemblages containing this raw material.

6. Conflict of Interest

The authors declare that the research was conducted in the absence of any commercial or financial relationships that could be construed as a potential conflict of interest.

7. Author Contributions

V.R. and R.O. conceived and designed the research and the experiments. R.O. performed the experiments and the wear analysis. V.R. and R.O. wrote and edited the paper. V.R. acquired funding and supervised the work.

8. Funding

The University of Liège generously provided funding for this research through the ARC (Concerted Research Actions) grant "GLUE". V. Rots is also indebted to the Fund for Scientific Research (F.R.S.-FNRS; DR).

9. Acknowledgments

We extend our gratitude to the TraceoLab team for their invaluable assistance and guidance throughout the process. Special thanks go to Christian Lepers for his expertise in producing experimental samples and for sharing his insights into the use of adhesives, and to Justin Coppe for thrusting the spears.

10. Data Availability Statement

All datasets [GENERATED/ANALYZED] for this study are published with in this article.

11. References

Aleo, A., 2023. Comparing the Formation and Characteristics of Use-Wear Traces on Flint, Chert, Dolerite and Quartz. Lithic Technol. 48, 130–148. https://doi.org/10.1080/01977261.2022.2103297

Archer, W., Presnyakova, D., Heinrich, S., Stahlschmidt, M.C., 2023. A Predictive Model for the Non-Destructive Assessment of Stone Age Silcrete Heat Treatment Strategies. J. Paleolit. Archaeol. 6, 14. https://doi.org/10.1007/s41982-023-00141-3

Asryan, L., Rots, V., 2024. Exploring Basalt: A Methodological Framework for Analysing Wear Traces on Basalt Tools. J. Archaeol. Method Theory 31, 1954–1983. https://doi.org/10.1007/s10816-024-09663-8

Berehowyj, L., 2013. Can Use-Wear Be Used To Identify Tuber Processing On Siliceous Stone? An Experimental Study From Australia. Aust. Archaeol. 77, 9–19. https://doi.org/10.1080/03122417.2013.11681975

Brown, K.S., Marean, C.W., Herries, A.I.R., Jacobs, Z., Tribolo, C., Braun, D., Roberts, D.L., Meyer, M.C., Bernatchez, J., 2009. Fire As an Engineering Tool of Early Modern Humans. Science 325, 859–862. https://doi.org/10.1126/science.1175028

Coppe, J., Lepers, C., Clarenne, V., Delaunois, E., Pirlot, M., Rots, V., 2019. Ballistic Study Tackles Kinetic Energy Values of Palaeolithic Weaponry. Archaeometry 61, 933–956. https://doi.org/10.1111/arcm.12452

Coppe, J., Rots, V., 2025. Let's cut to the chase and rely on fracture mechanics to identify projectile armatures. Archaeol. Anthr. Sci. 17, 73. https://doi.org/10.1007/s12520-025-02180-z

Coppe, J., Rots, V., 2017. Focus on the target. The importance of a transparent fracture terminology for understanding projectile points and projecting modes. Journal of Archaeological Science: Reports 12, 109–123. https://doi.org/10.1016/j.jasrep.2017.01.010

Delagnes, A., Schmidt, P., Douze, K., Wurz, S., Bellot-Gurlet, L., Conard, N.J., Nickel, K.G., Niekerk, K.L.V., Henshilwood, C., 2016. Early evidence for the extensive heat treatment of silcrete in the Howiesons Poort at Klipdrift Shelter (Layer PBD, 65 ka), South Africa. PLoS ONE 11, 1–27. https://doi.org/10.1371/journal.pone.0163874

Douze, K., Delagnes, A., Wurz, S., Henshilwood, C.S., 2018. The howiesons poort lithic sequence of klipdrift shelter, Southern Cape, South Africa. PLoS ONE 13, 1–24. https://doi.org/10.1371/journal.pone.0206238

Hayes, E., Pardoe, C., Fullagar, R., 2018. Sandstone grinding/pounding tools: Use-trace reference libraries and Australian archaeological applications. Journal of Archaeological Science: Reports 20, 97–114. https://doi.org/10.1016/j.jasrep.2018.04.021

Henshilwood, C., d'Errico, F., Vanhaeren, M., Niekerk, K. van, Jacobs, Z., 2004. Middle Stone Age Shell Beads from South Africa. Science 304, 404–404. https://doi.org/10.1126/science.1095905

Henshilwood, C., D'errico, F., Marean, C.W., Milo, R.G., Yates, R., 2001. An early bone tool industry from the Middle Stone Age at Blombos Cave, South Africa: Implications for the origins of modern human behaviour, symbolism and language. Journal of Human Evolution 41, 631–678. https://doi.org/10.1006/jhev.2001.0515

Hilbert, Y.H., Clemente-Conte, I., Crassard, R., Charloux, G., Guagnin, M., AlSharekh, A.M., 2022. Traceological analysis of lithics from the Camel Site, al-Jawf, Saudi Arabia: an experimental approach to identifying mineral processing activities using silcrete tools. Archaeol. Anthr. Sci. 14, 93. https://doi.org/10.1007/s12520-022-01559-6

Hodgskiss, T., 2020. Ochre Use in the Middle Stone Age. Oxford Research Encyclopedia of Anthropology. https://doi.org/10.1093/acrefore/9780190854584.013.51

Hodgskiss, T., 2013. Ochre use in the Middle Stone Age at Sibudu, South Africa: Grinding, rubbing, scoring and engraving. Journal of African Archaeology 11, 75–95. https://doi.org/10.3213/2191-5784-10232

Igreja, M., 2008. Use - wear analysis of non - flint stone tools using DIC microscopy and resin casts : a simple and effective technique.

Igreja, M., Porraz, G., 2013. Functional insights into the innovative Early Howiesons Poort technology at Diepkloof Rock Shelter (Western Cape, South Africa). Journal of Archaeological Science 40, 3475–3491. https://doi.org/10.1016/j.jas.2013.02.026

Kamminga, J., 1982. Over the edge: Functional analysis of Australian stone tools. Occasional Papers in Anthropology.

Key, A., Pargeter, J., Schmidt, P., 2021. Heat treatment significantly increases the sharpness of silcrete stone tools. Archaeometry 63, 447–466. https://doi.org/10.1111/arcm.12619

Lemorini, C., Plummer, T.W., Braun, D.R., Crittenden, A.N., Ditchfield, P.W., Bishop, L.C., Hertel, F., Oliver, J.S., Marlowe, F.W., Schoeninger, M.J., Potts, R., 2014. Old stones' song: Use-wear experiments and analysis of the Oldowan quartz and quartzite assemblage from Kanjera South (Kenya). J. Hum. Evol. 72, 10–25. https://doi.org/10.1016/j.jhevol.2014.03.002

Liu, J.-Y., Chen, H., 2016. An experimental case of wood-working use-wear on quartzite artefacts. Doc. Praehist. 43, 507–514. https://doi.org/10.4312/dp.43.27

Moss, E., 1983. The functional analysis of flint implements: pincevent and pont d'Ambon: two case studies from the French final Palaeolithic. BAR Publishing.

Mourre, V., Villa, P., Henshilwood, C., 2010a. Early use of pressure flaking on lithic artifacts at Blombos Cave, South Africa. Science 330, 659–662. https://doi.org/10.1126/science.1195550

Mourre, V., Villa, P., Henshilwood, C.S., 2010b. Early Use of Pressure Flaking on Lithic Artifacts at Blombos Cave, South Africa. Science 6004.

Munt, S., Fullagar, R., Murray, R., Corporation, M.A., 2023. Experimental use-wear patterns on silcrete, bottle glass and porcelain plate tools. Aust. Archaeol. 89, 188–205. https://doi.org/10.1080/03122417.2023.2215473

Murray, J., Harris, J., Oestmo, S., Martin, M., Marean, C., 2020. A new approach to identify heat treated silcrete near Pinnacle Point, South Africa using 3D microscopy and Bayesian modeling. J. Archaeol. Sci.: Rep. 34, 102622. https://doi.org/10.1016/j.jasrep.2020.102622

Ollé, A., Pedergnana, A., Fernández-Marchena, J.L., Martin, S., Borel, A., Aranda, V., 2016. Microwear features on vein quartz, rock crystal and quartzite: A study combining Optical Light and Scanning Electron Microscopy. Quat. Int. 424, 154–170. https://doi.org/10.1016/j.quaint.2016.02.005

Pargeter, J., Schmidt, P., 2020. 'Simple' surface-fire heat treatment significantly improves silcrete flake quality and flaking efficiency. J. Archaeol. Sci.: Rep. 30, 102203. https://doi.org/10.1016/j.jasrep.2020.102203

Pedergnana, A., Ollé, A., 2017. Monitoring and interpreting the use-wear formation processes on quartzite flakes through sequential experiments. Quat. Int. 427, 35–65. https://doi.org/10.1016/j.quaint.2016.01.053

Porraz, G., Texier, P.J., Archer, W., Piboule, M., Rigaud, J.P., Tribolo, C., 2013. Technological successions in the Middle Stone Age sequence of Diepkloof Rock Shelter, Western Cape, South Africa. Journal of Archaeological Science 40, 3376–3400. https://doi.org/10.1016/j.jas.2013.02.012

Porraz, G., Texier, P.-J., Rigaud, J.-P., Parkinton, J., Poggenpoel, C., Roberts, D., 2008. Preliminary Characterization of a Middle Stone Age Lithic Assemblage Preceding the “Classic” Howieson’S Poort Complex At Diepkloof Rock Shelter, Western Cape Province, South Africa. Goodwin Series 10, 105–121. https://doi.org/10.2307/40650022

Rots, V., Plisson, H., 2014. Projectiles and the abuse of the use-wear method in a search for impact. Journal of Archaeological Science 48, 154–165. https://doi.org/10.1016/j.jas.2013.10.027

Schmidt, P., Mackay, A., 2016. Why was silcrete heat-treated in the Middle Stone Age? An early transformative technology in the context of raw material use at Mertenhof rock shelter, South Africa. PLoS ONE 11, 1–16. https://doi.org/10.1371/journal.pone.0149243

Schmidt, P., Porraz, G., Bellot-Gurlet, L., February, E., Ligouis, B., Paris, C., Texier, P.J., Parkington, J.E., Miller, C.E., Nickel, K.G., Conard, N.J., 2015. A previously undescribed organic residue sheds light on heat treatment in the Middle Stone Age. Journal of Human Evolution 85, 22–34. https://doi.org/10.1016/j.jhevol.2015.05.001

Schmidt, P., Porraz, G., Slodczyk, A., Bellot-gurlet, L., Archer, W., Miller, C.E., 2013. Heat treatment in the South African Middle Stone Age: temperature induced transformations of silcrete and their technological implications. J Archaeol Sci 40, 3519–3531. https://doi.org/10.1016/j.jas.2012.10.016

Schmidt, P., Stynder, D., Conard, N.J., Parkington, J.E., 2020. When was silcrete heat treatment invented in South Africa? Palgrave Commun. 6, 73. https://doi.org/10.1057/s41599-020-0454-z

Schoville, B.J., Wilkins, J., Ritzman, T., Oestmo, S., Brown, K.S., 2017. The performance of heat-treated silcrete backed pieces in actualistic and controlled complex projectile experiments. Journal of Archaeological Science: Reports 14, 302–317. https://doi.org/10.1016/j.jasrep.2017.05.053

Stephenson–Gordon, G., 2021. The durability of silcrete flakes: An experimental analysis on the rate of use–wear formation for fine–grained silcrete flakes, in: Kelly, D., Frankel, D., Lawrence, S., Spry, C., Foley, E. (Eds.), An Experimental Study Assessing the Utility of Heat Treating Silcrete for Thepurposes of Working Wood and Animal Hidepurposes of Working Wood and Anim. pp. 85–93.

Texier, P.J., Porraz, G., Parkington, J., Rigaud, J.P., Poggenpoel, C., Miller, C., Tribolo, C., Cartwright, C., Coudenneau, A., Klein, R., Steele, T., Verna, C., 2010. A Howiesons Poort tradition of engraving ostrich eggshell containers dated to 60,000 years ago at Diepkloof Rock Shelter, South Africa. Proceedings of the National Academy of Sciences of the United States of America 107, 6180–6185. https://doi.org/10.1073/pnas.0913047107

Toddhunter, C., 2021. An experimental study assessing the utility of heat treating silcrete for thepurposes of working wood and animal hidepurposes of working wood and anim.

Tydgadt, L., Rots, V., 2025. Finding your strong points: exploring the design and resilience of barbed composite weapons. Archaeol. Anthr. Sci. 17, 112. https://doi.org/10.1007/s12520-025-02177-8

Tydgadt, L., Rots, V., 2022. Stick to it! Mechanical performance tests to explore the resilience of prehistoric glues in hafting. Archaeometry 64, 1252–1269. https://doi.org/10.1111/arcm.12779

Watson, S., 2025. Silcrete use and heat treatment in the middle stone age at Nelson Bay cave, South Africa. Archaeol. Anthr. Sci. 17, 126. https://doi.org/10.1007/s12520-025-02240-4

Webb, J., Finlayson, B., Cochrane, G., Doelman, T., Domanski, M., 2013. Silcrete quarries and artefact distribution in the Central Queensland Highlands, Eastern Australia. Archaeol. Ocean. 48, 130–140. https://doi.org/10.1002/arco.5014